

CONTRIBUTED PAPERS

AN INTRODUCTION TO IN-HOUSE EXAFS FACILITIES

YASUO UDAGAWA

Institute for Molecular Science, Okazaki, Aichi 444, Japan

Requirements for EXAFS spectrometers with a conventional rotating anode X-ray generator are discussed and the principle of a focusing spectrometer to substantiate those requirements is described. Two examples of in-house EXAFS spectrometers are presented and their performances as well as some applications are reported.

1. Introduction

EXAFS is an acronym of extended X-ray absorption fine structure. It refers to oscillatory structures which appear in the high energy side of characteristic X-ray absorption edges of elements. It appears only when the absorbing atoms are in a condensed phase, and reflects the local structure around the atoms. Experimentally, EXAFS function χ is defined by $\chi = (\mu - \mu_0)/\mu_0$, where μ is the observed absorbance and μ_0 is the absorbance of the element when the atom is isolated.

The origin of EXAFS can simply be explained in the following manner. Each element has its characteristic absorption energy in the X-ray region. When an atom absorbs an X-ray photon, a photoelectron emanates from the atom as an outgoing wave. If the

atom is in a condensed phase, the photoelectron will be backscattered by surrounding atoms. As a result, an interference effect takes place.

It is just like a fish (atom) in a pond excited by a bait (X-ray) jumps up and makes a ripple (outgoing wave) as shown in Fig. 1. If there is a rock nearby, the ripple is reflected back (backscattered wave), making a complicated pattern. By the choice of the bait the kind of fish may be identified, and it should in principle be possible to analyze the pattern to obtain the distance between the fish and the rock.

In quantum mechanics, absorption is described as a transition from an initial to a final state. In one electron approximation the electron involved in X-ray absorption is described by a wavefunction of an inner shell in the initial state. In the final state it is described by a wavefunction expressed as a superposition of outgoing and backscattered waves. Assuming a single scattering of plane wave, the following equation for EXAFS can be derived by employing quantum theory of scattering [1], [2],

$$\chi(k) = \sum_j \frac{N_j}{kr_j^2} F_j(\pi, k) \times \exp(-2k^2\sigma_j^2 - 2r_j/\lambda) \sin(2kr_j + \alpha_j(k)) \quad (1)$$

where k is the photoelectron wavevector, N_j is the number of atoms in the j -th shell, r_j is the distance from the central absorbing atom to atoms in the j -th shell, $F_j(k)$ is the scattering amplitude, σ_j is Debye-Waller factor, and $\alpha_j(k)$ is the phase shift. By Fourier transforming Eq. 1, radial structure function, whose abscissa and ordinate represent interatomic distance and coordination number, can be obtained. Further,

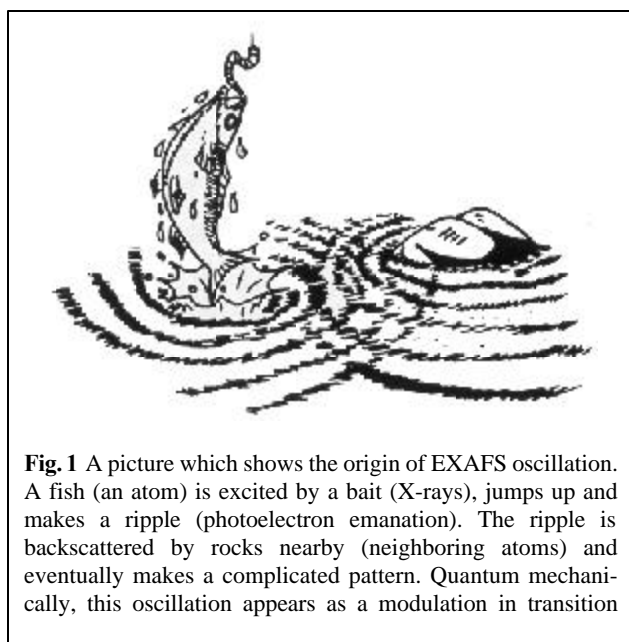


Fig. 1 A picture which shows the origin of EXAFS oscillation. A fish (an atom) is excited by a bait (X-rays), jumps up and makes a ripple (photoelectron emanation). The ripple is backscattered by rocks nearby (neighboring atoms) and eventually makes a complicated pattern. Quantum mechanically, this oscillation appears as a modulation in transition

inverse Fourier transform followed by least-squares fitting may be employed to refine structural parameters. Backscattering amplitudes and phase factors which appear in Eq. 1 can be theoretically calculated or empirically estimated from standard materials and their effects can be corrected in the course of the analysis [3]. It is evident from the principle of EXAFS that materials studied by EXAFS does not necessarily have a periodic structure; local structure of a selected element in amorphous materials can be probed. This is the reason why EXAFS has become so popular in recent years.

EXAFS experiment being just an absorption measurement in the X-ray region, apparently it looks very easy to do. It is, however, not true. Because EXAFS oscillation is less than 10% of background absorption and structural parameters can be obtained only after Fourier transformation, very accurate (better than 0.1%) absorbance measurement must be made, which is not an easy task. Since the statistical error is proportional to the square root of photon numbers, it is necessary to collect much more than a million count at each data point to achieve this goal.

What is more, everything from nonlinearity of detectors to slight changes in sample conditions degrades the quality of spectra to make results unreliable.

Synchrotron radiation (SR) is an ideal source for EXAFS studies; intense, directional, and spectrally monotonous [4]. Therefore it is no wonder that EXAFS studies have grown with the development of SR facilities whose energies are high enough to supply hard X-rays. Unfortunately the number of such SR facilities is limited and consequently a majority of workers must await in a long queue to have an access to an SR EXAFS station. Under these circumstances demands for an EXAFS spectrometer of laboratory scale have highly increased. To discuss and review possibilities and limitations of laboratory EXAFS measurement a workshop was organized by Prof. Stern at University of Washington in 1980 [5]. Since then a great deal of efforts have been made to develop in-house EXAFS facilities. In early days of the development spectrographs employing one dimensional detector have been tried, but now it is a general agreement that spectrometers with a bent monochromator crystal employing Rowland circle

Table 1 A comparison of laboratory EXAFS facilities.

Authors (year) and ref #	Monochromating crystal	Rowland radius (mm)	Detector*	Number of motors	Features of Scanning
1. Knapp et al. (1978) [7]	Johansson Ge (200)	200	SC		Source and detector move on a fixed Rowland circle
2. Cohen et. al. (1980) [8]	Johansson LiF (220)	350	PC+IC	1	Linear spectrometer guided by arms
3. Gregopoulos et al. (1981) [9]	Johann Si (400)	200	PC+PC	1	Linear spectrometer guided by arms
4. Khalid et al. (1982) [10]	Johansson Si (311)	500 (adaptable)	IC+IC	4	Computer controlled pulse motors without mechanical guides
5. Williams (1983) [11]	Johansson Ge (111)	300-500	IC-IC or SC	1	X'tal and detector move on a fixed Rowland circle
6. Thulke et al. (1983) [12]	Johansson Ge(311), Si(111), Si(311)	352 (adaptable)	IC+IC	4	Computer controlled pulse motors without mechanical guides
7. Tohji et al. (1983) [13]	Johansson Ge(220), Ge(311), LiF(220)	320	IC+SSD	2	Linear spectrometer guided by arms; for details, see text
8. Brinkgreve et al. (1984) [14]	Johann Si(400) Johansson Si(111), Si(311), Ge(311)	500	IC+IC	1	Linear spectrometer guided by arms
9. Sano et al. (1984) [15]	Johann LiF(200)	275	PC+PC	1	Linear spectrometer guided by an arm
10. Yacoby et al. (1987) [16]	Si(400), Ge(533)	250-750	IC		Huber goniometer mounted on lathe table
11. Tohji et al. (1988) [17]	Johansson Ge(333), Ge(440), LiF(200)	320	IS+SC	4	Two crystal monochromator; for details see text

* SC = scintillation counter; PC: proportional counter; IC: ionization chamber; SSD: solid state detector

focusing geometry are superior. In Table 1 main specifications of bent crystal monochromators published so far are surveyed [6]-[17]. Various aspects of bent crystal spectrometers have already been reviewed in refs. 5 and 6. In this article features of in-house EXAFS spectrometers are described, two examples used in our laboratory are presented, and their performances are reported.

2. Characteristics of Laboratory X-ray Sources and Spectrometers

2.1 Source

There are two types of conventional X-ray generators; sealed tubes and rotating anodes. The latter is preferable because it can supply about an order of magnitude more intense X-ray fluxes. Though, even with the rotating anode X-ray generator, photon flux available is about three orders of magnitude weaker than that from synchrotron facilities. What is more, unlike X-rays from SR, "white" X-rays produced by bremsstrahlung is not really white at all but are overlapped with many intense characteristic lines arising from the target material as well as impurities on it. Especially, tungsten gradually accumulates on the target because of slow evaporation from the filament and produces many strong lines between 7 and 12 keV, where the first row transition elements have absorption edges. Large intensity variation of the incident flux due to these characteristic lines may make serious distortions of spectra because of finite dynamic range of detectors.

In-house EXAFS spectrometers must be designed by taking these features of the source into consideration; the X-rays must be collected as efficiently as possible to overcome the low intensity, the flux must be stabilized by a feedback system, and the detectors must be fast enough. In addition, X-rays due to harmonic reflections from monochromator crystals are always contaminated at both SR and laboratories, thus the desired order of reflection must be picked out by discriminating higher or lower orders.

2.2 Monochromator

A Rowland circle geometry employing a bent crystal is the best choice to achieve high photon flux. In this configuration, three parts, the source, the monochromator crystal, and the exit slit, should be on the circle whose diameter is the half of the radius of the crystal, and to scan energy the incident angle must be continuously changed while keeping Bragg's condition. Several methods have been presented to fulfill the above requirements as is shown in Table 1.

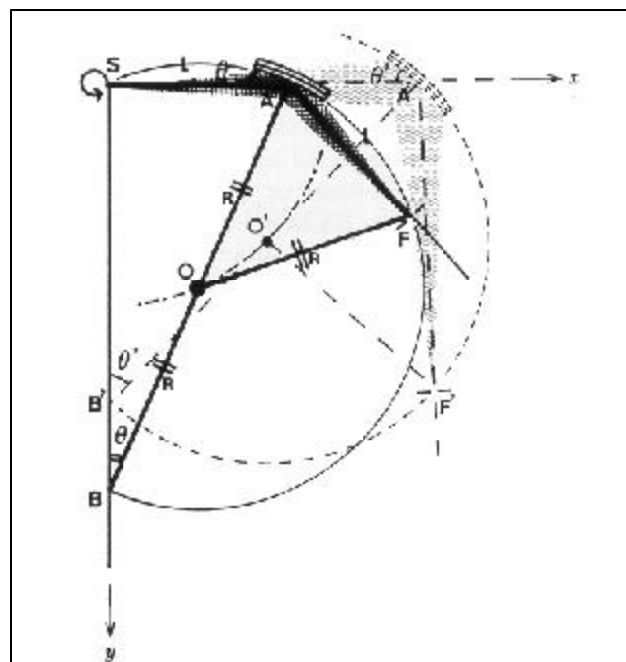


Fig. 2 A principle of a linear spectrometer with a bent crystal. Two positions of the spectrometer are shown. S: X-ray source; A: center of the monochromator crystal; F: exit slit; O: center of Rowland circle. X-ray source is fixed and the distances SA is always kept to be the same as AF and X-ray energy is scanned by changing the distances SA and AF by stepping motors. The chain is the trajectory of O as X-ray energy is

In every method one of the three is fixed and the others move. Employing a rotating anode X-ray generator the X-ray source is preferred to be fixed because of its weight.

Fig. 2 shows the principle of a spectrometer which satisfy the above requirements and sometimes called a linear spectrometer. The positions for two different energies are shown. X-ray source S is the only fixed point on the Rowland circle. The crystal is mounted at one end of a bar of $2R$ in length and is oriented such that the crystal normal is parallel to the bar. Each end of the bar slides along x or y axis, and the middle of this bar (O) makes the center of the Rowland circle and moves along a circle with radius R around S. The slit F moves on a lead whose end is fixed to the crystal center and allowed to rotate about that point. The direction of this lead is determined by another bar which connects O and F. The distance between S and A is kept to be the same as A and F, and is continuously changed with a screw motions by stepping motors. Then, the triangle SAO is always the same as AOF, thus Bragg's condition being always fulfilled and the wavelength λ of the photons reflected by a monochromator crystal with lattice spacing d is

linearly dependent on the distance l (SA and AF) in the following manner;

$$n\lambda = 2d \sin \theta = d/R$$

Here n is the order of reflection. Incidentally, instead of a bar AB of $2R$ in length, another bar with R in length which connects S and O may be used.

2.3 Monochromator Crystal

For Rowland circle with radius R , the crystal can be either Johann (simply bent to radius $2R$) or Johansson (bent as Johann and also ground with radius R). Optimal resolution without aberrations can be obtained by Johansson type crystal, although to manufacture an undistorted one is difficult. As is shown in Table 1, several index planes of LiF, Si, and Ge have been employed by the previous workers. Main concern in selecting a crystal lies in resolution and brightness. According to Knapp and Georgopoulos [5], [9], the resolution of the crystal with lattice constant d at energy E is expressed by the following equation

$$\Delta E = \frac{E^3(2d)^2}{8RC^2} \left[(W_s + W_f)^2 + \left(\frac{h^2}{8R}\right)^2 + \left(\frac{CE^2 \ln 2}{Kd}\right)^2 \right]^{1/2} \quad (2)$$

Here C is a constant (12.396 eV Å), W_s and W_f are the widths of the X-ray source and the exit slit, h is the slit height, and absorption coefficient μ is approximated to be $\mu = K/E^3$. This equation states that the resolution is proportional to $(2d)^2$, thus by using high index crystal planes with small d the resolution can be improved. The third term has a very strong energy dependence and become significant at higher energies where the absorption is lower. Hence, Si and LiF are not adequate at high energies. Calculated resolution curves for various monochromator crystals can be found in literatures [5], [9], [12], [18].

2.4 Detectors

Several kinds of detectors have been employed as shown in Table 1. Out of these, ionization chamber does not have energy resolution, and cannot discriminate against higher harmonics but has an excellent linearity over wide ranges. Scintillation counters, gas proportional counters, and solid state detectors have a variety of energy resolution and speed. If the X-ray that impinges the detector is monochromatic and free from any harmonics, ionization chamber is the best choice because of its high dynamic range and low cost. If not, an appropriate detector should be chosen according to conditions. It is highly preferable to detect I and I_0 simultaneously to avoid degradation of spectra due to fluctuations of X-ray flux.

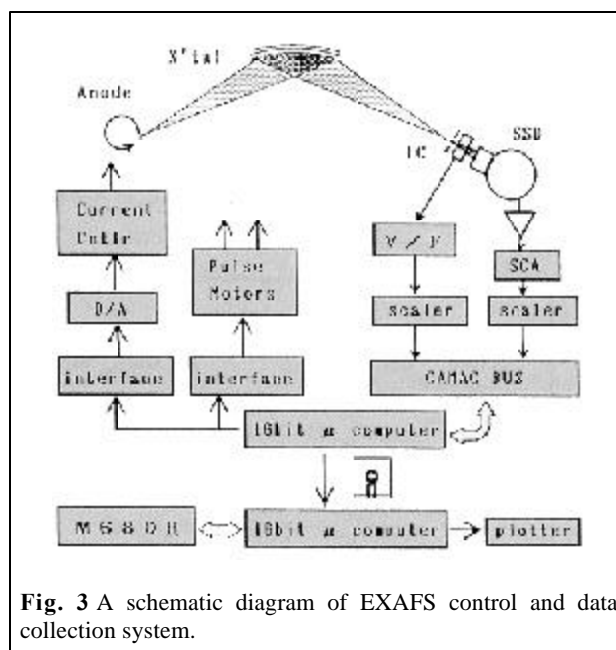


Fig. 3 A schematic diagram of EXAFS control and data collection system.

2.5 Data Collection System

Since it takes typically from several hours to a day to collect an EXAFS data of a sample with a moderate concentration, an automatic data acquisition system is a must in in-house EXAFS systems. Thanks to rapid development of microcomputer in the recent years, it can be accomplished at rather low cost now. An example of such a system is shown in Fig. 3. In this system a microcomputer controls scanning, data acquisition, and source stabilization. Data collected are transferred to the main computer of a computing center through TSS and the analysis is carried out while the next measurement is in progress. I_0 signal is always monitored and the X-ray intensity is stabilized with a feedback system by controlling the current of the X-ray generator.

3. Example of Laboratory EXAFS Spectrometers and Their Performances

3.1 One Crystal Monochromator

An EXAFS spectrometer which is based on the principle shown in Fig. 2 and is equipped with the detection system and electronics of Fig. 3 has been previously described in detail [13]. This system uses a semitransmitting ionization chamber and a pure Ge solid state detector to detect I_0 and I , respectively. Contamination of higher harmonics is avoided by maintaining the source voltage below the twice of the energy of interest. In case higher harmonics should be used for heavy elements whose characteristic absorptions lie > 15 keV, both I_0 and I are detected with the

same SSD, by inserting a sample and reference across the X-ray path alternatively.

Resolving power of this system depends on the monochromator crystal, slit width, and energy. Resolving power as measured by FWHM of Cu $K\alpha$ lines at about 8 keV is 6 eV with Ge(220) crystal and slit width of 200 μ . Ge(440) gives much better resolution and sharp features near absorption edge instead of characteristic lines must be employed for the estimation of the resolution. Fig. 4 shows near edge absorption spectra of some copper compounds by the use of

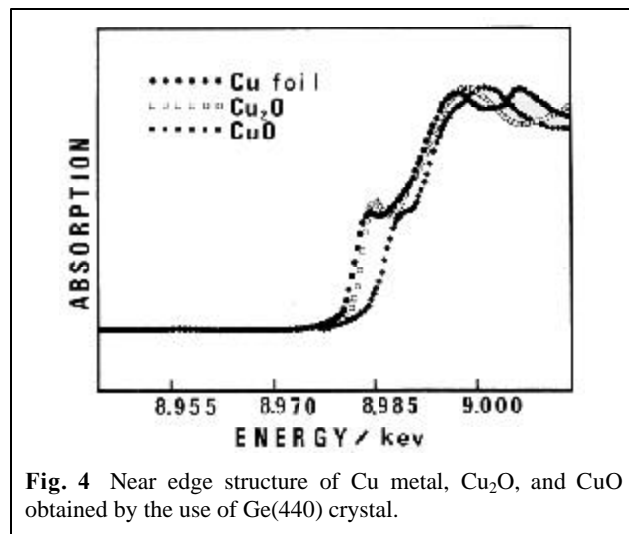


Fig. 4 Near edge structure of Cu metal, Cu_2O , and CuO obtained by the use of Ge(440) crystal.

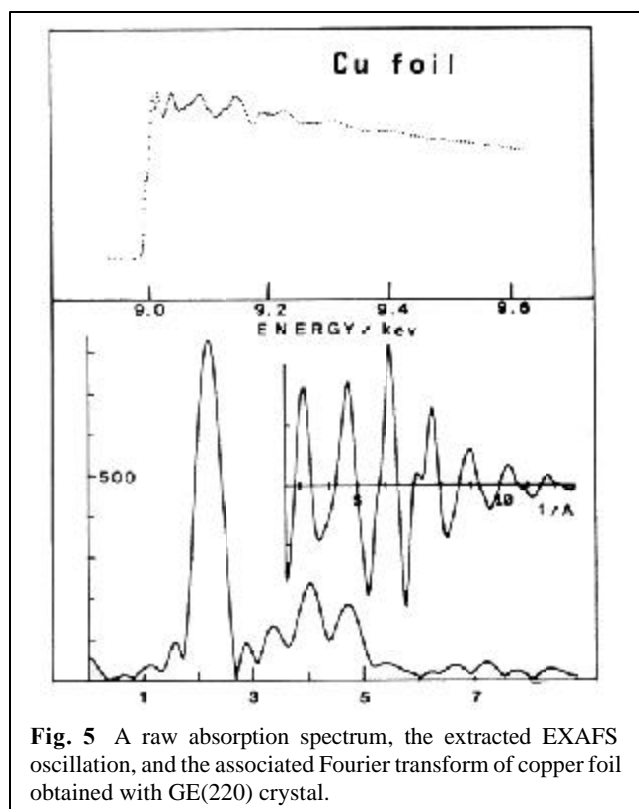


Fig. 5 A raw absorption spectrum, the extracted EXAFS oscillation, and the associated Fourier transform of copper foil obtained with Ge(220) crystal.

Ge(440) reflection. Since the kink at the absorption edge of copper metal is evident, the resolution is estimated to be about 2eV. With this resolution differences in near absorption edge structure by different copper environments are clearly observed. An XANES (X-ray Absorption Near Edge Structure) study with this system on catalysts containing copper has been reported [18]. The resolution decreases with the increase in energy due to the third term of Eq. 2, and therefore higher order reflections must be employed at high energy. For example, at about 17 keV where Mo, has $K\alpha$ lines the resolution as measured by FWHM is 15 and 7 eV with Ge(440) and with Ge(660) crystals, respectively.

As an example of EXAFS spectrum taken with this system, an absorption, the extracted oscillation, and the associated Fourier transform of copper foil are shown in Fig. 5. This was obtained with Ge(440) crystal in 8 hours. Peaks characteristic of fcc metals are clearly observed.

For EXAFS studies on the compounds containing first row transition metals either a Ge(220) or a Si(220) crystal is usually employed because of their high efficiency. In Fig. 6(a) shown is a raw EXAFS spectrum, Ni absorption after subtracting background absorption, and the extracted EXAFS oscillation of nickel catalyst supported on silica. Since Ni concentration is as low as 1 wt.%, background absorption due to the support dominates. In spite of the large background absorption, S/N ratio is so good that the extracted oscillation almost perfectly reproduces the features of Ni metal EXAFS. By introducing CO onto this catalyst, CO molecules are first adsorbed on the metal surface and then gradually $\text{Ni}(\text{CO})_4$ is formed. In Fig. 6(b) shown is the raw spectrum, Ni absorption, and an extracted EXAFS oscillation at an intermediate stage. A decrease of the amplitude and a considerable change at low k region which comes from Ni-C interaction are evidenced.

From the examples above, it must be evident that the system described here can supply EXAFS spectra of quality and this has been successfully applied so far for the structural study of various materials containing Mn through Rh [18]-[24].

3.2 A Double Crystal Monochromator

At high energy region higher order harmonics such as Ge(444) or Ge(660) must be used in order to get sufficiently high resolution. In that case an ionization chamber cannot be used to detect I_0 with the monochromator described above, because the lower as well as the higher order reflections always

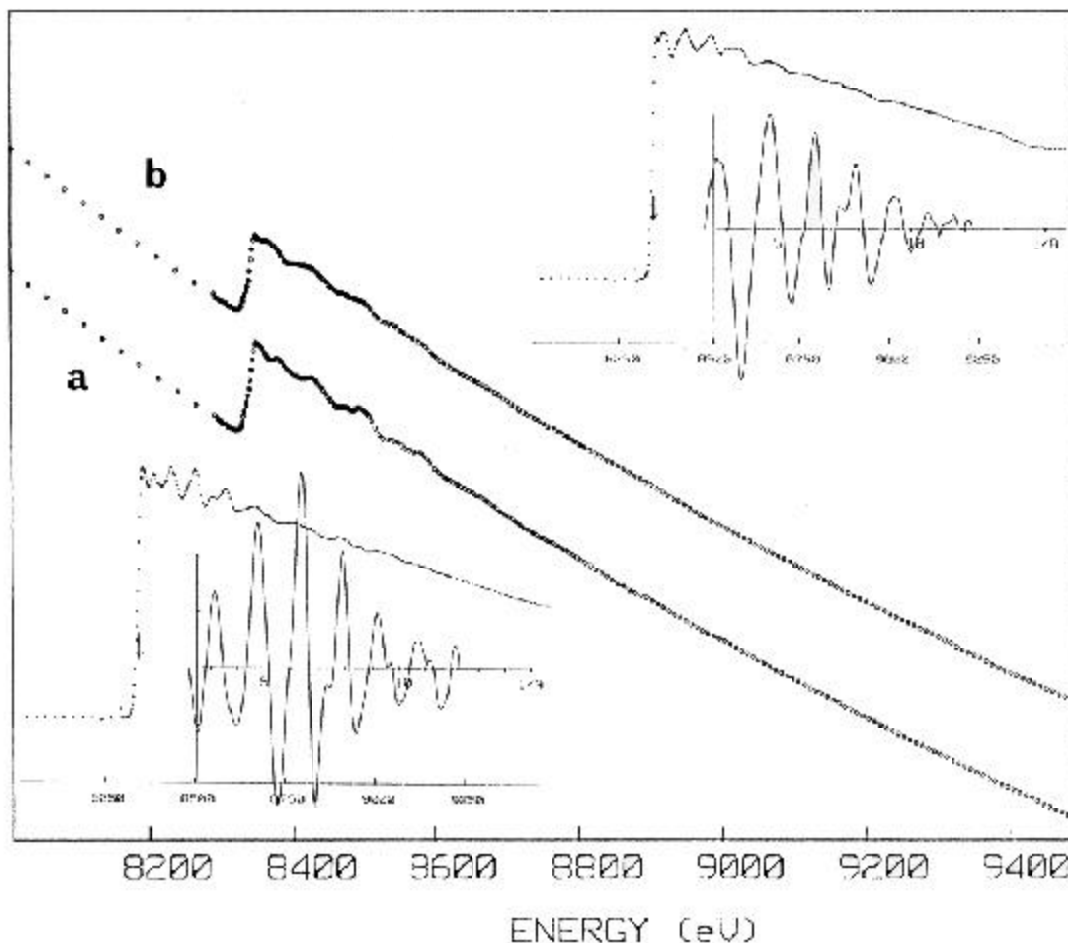


Fig. 6 Raw X-ray absorption spectra, subtracted Ni absorption, and extracted EXAFS of Ni catalyst (1 st. %) Supported on silica (a) and those of the catalyst after CO admission (b).

accompany. Thus, in the spectrometer described in 3.1, I and I_0 must be measured alternatively by an SSD instead of simultaneous detection. Studies on Ru, Rh, and Zr have been successfully carried out by this method [18], [22]. Although an absolute absorbance can be obtained, however, the quality of data is subject to the fluctuation of the source during collection periods of photons for I and I_0 and it takes at least twice the time for a measurement.

To overcome this drawback, a double crystal monochromator has been developed [17], whose schematic diagram is shown in Fig. 7. This monochromator consists of two monochromators of similar design having the same Rowland radius of 320 mm, and features a complete discrimination against X-rays from reflections of unwanted orders. Resolution is determined by the first monochromator, thus being the same as the single crystal monochromator described above, and the second one serves just as an order sorter. To do so crystals with different extinction rule

have to be combined. For example, when Ge(333) reflection is used at 24 keV, X-rays of 8, 32, 40, and 56 keV originating from Ge(111), Ge(444), Ge(555), and Ge(777) reflections accompany. In this case LiF(200) or (220) crystal is suited in the second monochromator, because then only the X-rays reflected by Ge(333) plane can be picked out. In principle, X-rays of 72 keV by Ge(999) reflection can contaminate, but in practice they do not exist at all because the source voltage is usually much lower than 70 kV. X-rays being free from unnecessary reflections, ionization chambers can be used to detect both I and I_0 in this monochromator.

To show the quality of data obtained with this spectrometer, Mo EXAFS of a commercially available hydrodesulfurization catalyst Co-Mo/ γ -Al₂O₃ (Mo content 10 wt.%) in sulfided form is shown in Fig. 8, as well as the associated Fourier transform. A combination of Ge(440) and LiF(220) was employed

in this measurement. A long oscillation is observed up to $k = 14 \text{ \AA}^{-1}$, and two peaks due to Mo-S and Mo-Mo appear in the transform. This resembles to the features of MoS_2 , but the relative intensity is not the same, offering a clue to understand the Mo environment of

this industrially important catalyst. This system has so far been applied for studies of catalysts containing Ru and Mo [25] [26].

4. Conclusion

In-house EXAFS measurement has a definite advantage over that at SR; a fast implementation of an idea by a timely experiments, eventually leading to new ideas which may be immediately tested by experiments which follows. Prof. Stern called it an iterative innovativeness [5]. Owing to recent technical improvements it is now possible to obtain EXAFS data of sufficient quality with laboratory EXAFS apparatus as has been shown in the previous section. Certainly various kinds of work can not be carried out with in-house EXAFS facilities; intense X-rays from SR is absolutely necessary for time resolved EXAFS, fluorescence detection EXAFS on very dilute samples, surface EXAFS, and so on. For samples with moderate concentration, however, in-house EXAFS apparatus can supply data of sufficient quality and should become more popular as an analytical tool in the near future.

References

- [1] D. E. Sayers, E. A. Stern, and F. W. Lytle: Phys. Rev. Lett., **27** (1971), 1204.
- [2] E. A. Stern: Phys. Rev., **B10** (1974), 3017.
- [3] B. K. Teo: EXAFS: Basic Principles and Data Analysis, Springer-Verlag (1986).

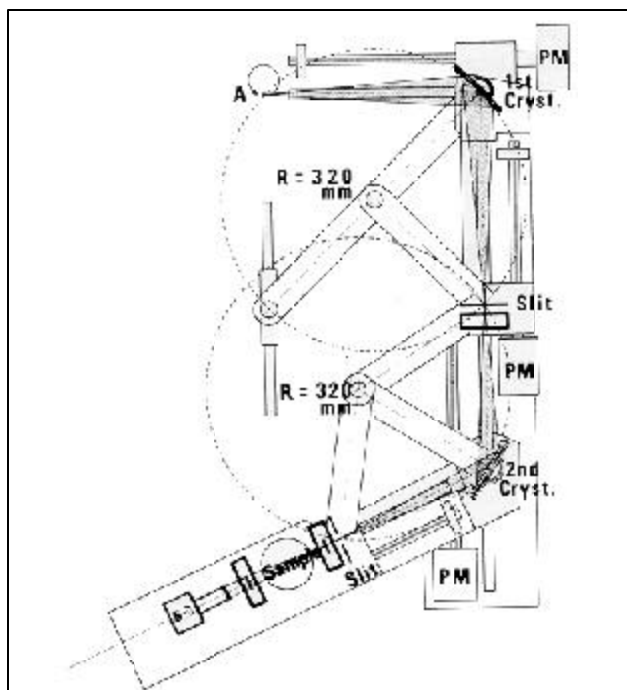


Fig. 7 A schematic diagram of the double crystal EXAFS monochromator. A: rotating anode; I: ionization chamber; I2: ionization chamber for alignment; SC: scintillation counter; PM: pulse motor. Dots represent two Rowland circles.

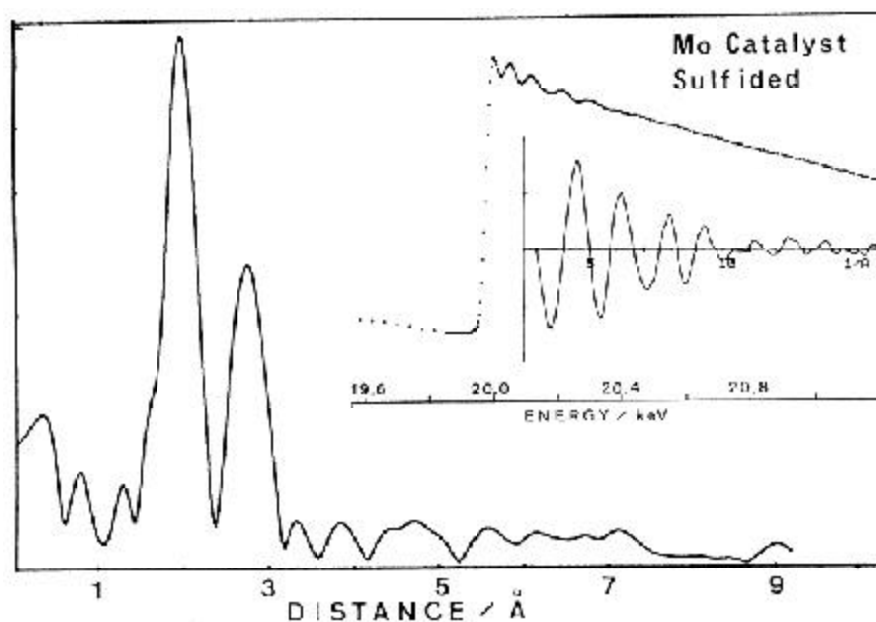


Fig. 8 Raw X-ray absorption, subtracted oscillation, and the associated Fourier transform of Mo EXAFS of Co-Mo/ γ - Al_2O_3 catalyst after sulfidation.

- [4] H. Winick and S. Doniach ed.: Synchrotron Radiation Research, Plenum (1980).
- [5] H. Stern ed.: Laboratory EXAFS Facilities-1980, AIP Conference Proceedings No. 64 (1980).
- [6] D. C. Koningsberger and R. Prins ed.: X-ray Absorption, John Wiley and Sons (1988).
- [7] G. S. Knapp, H. Chen, and T. E. Klippert: Rev. Sci. Instrum., **49** (1978), 1658.
- [8] G. C. Cohen, D. A. Fischer, J. Colbert, and N. J. Schevchik: Rev. Sci. Instrum., **51** (1980), 273.
- [9] P. Georgopoulos and G. S. Knapp: Appl. Cryst., **14** (1981), 3.
- [10] S. Khalid, R. Emlich, R. Dujari, J. Schultz, and J. R. Kazter: Rev. Sci. Instrum., **53** (1982), 22.
- [11] A. Williams: Rev. Sci. Instrum., **54** (1983), 193.
- [12] W. Thulke, R. Haensel, and P. Rabe: Rev. Sci. Instrum., **54** (1982), 1482.
- [13] K. Tohji, Y. Udagawa, T. Kawasaki, and K. Masuda, Rev. Sci. Instrum., **54** (1982), 1482.
- [14] M. Sano, T. Marumo, and H. Yamatera: Bull. Chem. Soc. Jpn., **57** (1984), 2757.
- [15] F. W. H. Kampers, F. B. M. Duivenvoorden, J. B. A. D. Zan Zon, P. Brinkgreve, M. P. A. Vieggers, and D. C. Koningsberger: Solid State Ionics, **16** (1985), 55.
- [16] Y. Yacoby, M. Brettschneider, and M. Bezalel, Rev. Sci. Instrum., **58** (1987), 588.
- [17] K. Tohji, Y. Udagawa, T. Kawasaki, and K. Mieno: Rev. Sci. Instrum., **59** (1988), 1127.
- [18] K. Tohji, Y. Udagawa, M. Harada, and A. Ueno: J. Chem. Soc. Jpn., (1986), 1559.
- [19] K. Tohji, Y. Udagawa, S. Tanabe, and A. Ueno: J. Am. Chem. Sec., **106** (1984), 612.
- [20] K. Tohji, Y. Udagawa, S. Tanabe, T. Ida, and A. Ueno: J. Am. Chem. Soc., **106** (1984), 5172.
- [21] K. Tohji, Y. Udagawa, T. Mizushima, and A. Ueno: J. Phys. Chem., **89** (1985), 5671.
- [22] Y. Udagawa, K. Tohji, Z. Z. Lin, T. Okuhara, and Y. Udagawa: J. de phys., **47** (1986), C8-249.
- [23] T. Ida, H. Tsuiki, A. Ueno, K. Toji, K. Iwai, and H. Sano: J. Catal., **106** (1987), 428.
- [24] T. Mizushima, K. Tohji, Y. Udagawa, M. Harada, M. Ishikawa, and A. Ueno: J. Catal., **112** (1988), 282.
- [25] N. Kakuta, K. Tohji, and Y. Udagawa: J. Phys. Chem., **92** (1988), 2587.
- [26] T. Mizushima, K. Tohji, and Y. Udagawa: J. Am. Chem. Soc., **110** (1988), 4459.